

On the water desorption of fruits: a case study of watermelon (*Citrullus Lanatus*)

Réda Khama^{1,2*}, Angélique Léonard²

(1. Department of Process Engineering, University of Batna 2, 5000 Batna, Algeria;

2. Department of Chemical Engineering, PEPs, University of Liège, 4000 Liège, Belgium)

Abstract: Studies on drying of the watermelon seeds or rinds are available, but not on drying of the fruit flesh. Data on the sorption of watermelon fruit (*Citrullus Lanatus*), which are useful and important when identifying optimal food drying and storage conditions, are also not available. Therefore, the main goal of this study is to investigate the water desorption behavior of watermelon using the dynamic method requiring the automated dynamic vapor sorption (DVS) technique based on a humidity-generating device. The moisture desorption isotherms are determined at three different temperatures (20 °C, 30 °C and 40 °C) over a relative humidity range of 0-80%. In addition, 11 different models are applied to the experimental data in order to select the appropriate desorption curve equation. The models are compared using the correlation coefficient, the coefficient of determination, the standard error, the reduced chi-squared, the mean bias error and the root mean square error; they are predicted by a non-linear regression analysis using the Curve Expert software and MS Excel computer program. The effect of the temperature on the constants of the found equation is also examined. Besides, the desorption isosteric heat of watermelon is determined using the Clausius-Clapeyron relation. Contrary to long times taken in the static method, the results show that 4.5 days are widely sufficient to reach the equilibrium via the DVS device. In addition, the obtained curves are of the type III and the Henderson model best fits the experimental data. In the interval 0.05-0.45 kg_{water}·kg_{dry matter}⁻¹ of equilibrium moisture, the values of the isosteric heat vary from 65.02 to 113.25 kJ mol⁻¹. Finally, the equation giving the isosteric heat of desorption v.s. the equilibrium moisture content is obtained.

Keywords: isotherms, drying, DVS, isosteric heat, experimental methodology, statistical analysis

Citation: Khama, R. and A. Léonard. 2024. On the water desorption of fruits: a case study of watermelon (*Citrullus Lanatus*). *Agricultural Engineering International: CIGR Journal*, 26(2): 238-252.

1 Introduction

The water sorption properties of solid materials are recognised as critical factors in determining their storage, stability, processing and application performance (Surface Measurement Systems Company, 2023). These properties are often represented by curves so-called sorption isotherms.

The thermodynamic concept of water activity is used in the drying applications through these sorption isotherms, which represent the water activity variation versus the moisture content variation of a body at equilibrium and at a defined constant temperature (Arlabosse et al., 2003; Garbalińska et al., 2017).

Knowing the moisture content of a product is insufficient to predict its stability, making it necessary to also know its water activity, a thermodynamic property describing the interactions between water molecules and the food matrix (Caballero-Cerón et al., 2015).

Received date: 2023-12-14 **Accepted date:** 2024-03-29

***Corresponding author: Réda Khama**, Ph.D Associate Professor, Department of Process Engineering, University of Batna 2, 5000 Batna, Algeria. Tel: +213 (0) 540640822, Emails: r.khama@univ-batna2.dz; redkhama@yahoo.fr.

Due to the complexity of the sorption phenomena, the isotherms of sorption cannot be predicted by the theory but must be experimentally established for every product. According to Djendoubi Mrad et al. (2013), the form of sorption isotherms is chiefly shaped by the structure and composition of the food material. In this way, the experimental determination is required because the methods of prediction are not able to simulate complex systems such as foods; temperature and pressure are also important factors (Djendoubi Mrad et al., 2013).

In order to extend the life duration of fruits, their water activity does not have to exceed 0.6 (Djendoubi Mrad et al., 2012). Then, it is essential to study the sorption characteristics of the dried products with water activities situated between 0 and 0.6 corresponding to the interval 0-60% of the air relative humidity (RH) (Djendoubi Mrad et al., 2012).

Numerous methods are available for the determination of water sorption isotherms (Basu et al., 2006). They can be divided into three categories, namely gravimetric, manometric and hygrometric (Deshmukh et al., 2017; Khama, 2016). The gravimetric method consists of fixing the pressure above the sample and measuring mass changes continuously or discontinuously in static or dynamic systems (Arlabosse et al., 2003; Basu et al., 2006; Khama, 2016).

In the static systems, the standardized saturated salt solution (SSS) method is the most common technique using thermostat jars filled with supersaturated saline solutions to maintain the desired RH (Basu et al., 2006). According to (Surface Measurement Systems Company, 2023), these manual jar methods have disadvantages: (i) The prolonged period of time (often many days and commonly many weeks) taken for the samples to reach equilibrium, which necessitates the use of large samples sizes (typically 10-100 g) to compensate for inherent analytical balance inaccuracies. (ii) Measurement errors associated with the required removal of samples from storage containers for periodic weighing often results in extraneous mass

loss or gain and thus contributing to measurement errors. (iii) The inability to measure the kinetics of water sorption/desorption uptake and release in real time limiting the utility of these static measurement techniques. (iv) The risk of mould formation or other sample contamination resulting from lengthy equilibration times and exposure to variable laboratory temperatures and humidities. In addition, the RH levels of the air around the samples, or even the water activity of the samples, are limited by the various available salt solutions (Yang et al., 2020).

In the dynamic systems, the sorption curves can be determined by dynamic vapor sorption (DVS), which is a modern technique producing sorption data with high accuracy under controlled conditions in a short period of time (Garbalińska et al., 2017; Arlabosse et al., 2003; Argyropoulos et al., 2011). Such a system is a real alternative, indeed the DVS Intrinsic is a highly sensitive, accurate and rapid means for automated determination of moisture sorption properties of solids (Surface Measurement Systems Company, 2023).

Haoua et al. (2015) examined the desorption isotherms of unblanched and blanched samples of potato exposed to a range of different temperatures (30 °C, 35 °C and 40 °C), using the DVS system. The obtained curves were of the type II in BDDT classification and the Oswin model best fitted the experimental data.

In the work of Goula et al. (2008), adsorption isotherms of tomato pulp spray dried in dehumidified air were determined at six temperatures (20 °C-70 °C), using a gravimetric technique. The experimental data were then fitted to six different models and the GAB model was found to be the most suitable to predict the adsorption isotherms. The isosteric heat of sorption was determined from the equilibrium adsorption data using the Clausius–Clapeyron equation and the isosteric heats of sorption were found to decrease exponentially with increasing moisture content. In addition, the enthalpy–entropy compensation theory was applied to the sorption isotherms and indicated an enthalpy controlled sorption process.

The research of Bingol et al. (2012), focused on the sorption behavior of two popular medium rice varieties (M202 and M206), in California by a new approach using DVS method for elucidating the differences in fissuring resistance. The moisture sorption isotherms of rough, brown and white rice and husk were determined at 25 °C over a water activity range of 0-0.98.

Although it was found that the sorption isotherms of different forms of M202 and M206 were similar, M202 absorbed and desorbed moisture faster than M206 which might make it more susceptible to fissuring. All obtained moisture sorption isotherms exhibited the sigmoid (Type II) shape and hysteresis was observed for all forms of rice.

Absorption curves obtained using DVS method were compared with the traditional SSS method. For all forms of rice, the maximum difference for equilibrium moisture content value between two methods was observed at 0 and 98% relative humidities, which was approximately 8%-11% and 7%-9%. Although at a single RH point equilibrium with DVS was attained much faster than SSS method, obtaining a full isotherm with more than 10 data points might make SSS method more feasible for low diffusion materials. Among the select equations to describe sorption behavior of different forms of rice, Peleg equation gave the best fit for all forms of rice.

According to Garbalińska et al. (2017), the investigation of Anderberg and Wadsö (2008) contains a comparison of the sorption isotherms of self-levelling flooring compounds with water to-binder ratio of about 1.0 and about 0.7 obtained by using the traditional method and the DVS method. Good compatibility of results was achieved for relative air humidity ranges between 10% and 95%.

Koocheki et al. (2007) mentioned that watermelon is a tropical fruit, which grows in almost all parts of Africa and South East Asia and, according to Kerje and Grum (2000), watermelon is a very rich source of vitamins and often used as an appetizer or snack, depending on how it is prepared.

According to Maoto et al. (2019), snacking has become a habit among consumers in recent years. These snacking trends together with unhealthy life styles may promote the formation of Reactive Oxygen Species (ROS) and free radicals which results in non-communicable diseases. As a result, replacing energy-dense snacks with fruits is encouraged. As a functional food, watermelon is a quintessential summer fruit loaded with phytochemicals.

The phytochemicals have been reported for their pharmacological activities and therapeutic properties such as analgesic, laxative, antiangiogenic, gastroprotective, hepatoprotective, antibacterial, antifungal, antimicrobial, antiulcer, antioxidant, and anti-inflammatory (Maoto et al., 2019).

Studies on the drying of watermelon seeds or rinds are available, but on the drying of the fruit itself are not. Data on water sorption of watermelon fruit is also not available. Therefore, in this work, the desorption isotherms and isosteric heat of watermelon are determined by a gravimetric method requiring the DVS. Indeed, regarding the previous published scientific works on watermelon, the theme of our research can be considered as the first one and the results as a novel contribution.

2 Materials and methods

2.1 Watermelon

Fresh watermelons are bought from a local market in Liège, Belgium at their commercial maturity according to some indices namely skin colour, shape, size and firmness. For each experiment, small samples are used with a thickness of about 2.5 mm and a mass varying between 33.49-36.23 mg.

2.2 Dynamic vapor sorption system (DVS)

The experiments are conducted within the PEPs (Products, Environment, and Processes) group at the University of Liège, Belgium. The sorption analyzer of water vapor (DVS) used is the last dynamic analyzer of water sorption of the outer measurement systems. The schematic of the main components of the DVS Intrinsic is shown in Figure 1, and the

specifications of this device are presented in Table 1.

The cantilever of the microbalance is continuously held in horizontal position by an applied moment. The electrical current used to uphold this moment is therefore an indirect measure of the mass loaded in the sample holder. The equipment is capable of keeping a stable temperature in the range 20 °C-40 °C. The RH of the air surrounding the loaded sample in the sample holder is controlled by mixing dry and water saturated air to a mixed air with a specified RH. Thus, in the range 0-98% RH all levels of RH are possible. This is an advantage over the traditional method with SSS, where the levels of RH were limited by the different available salt solutions (Engelund et al., 2010).

This type of DVS Advantage is capable of handling up to 4 g sample mass; however, for a highly hygroscopic material like fruits, a sample mass of around 20-50 mg is enough. The smaller the sample mass, the faster the data acquisition. However, in order to secure accuracy of the obtained results, sample masses below 1 g should be avoided. Using

the DVS introduces another parameter – the time-out. This parameter sets the maximum time spent at each RH level before moving up or down.

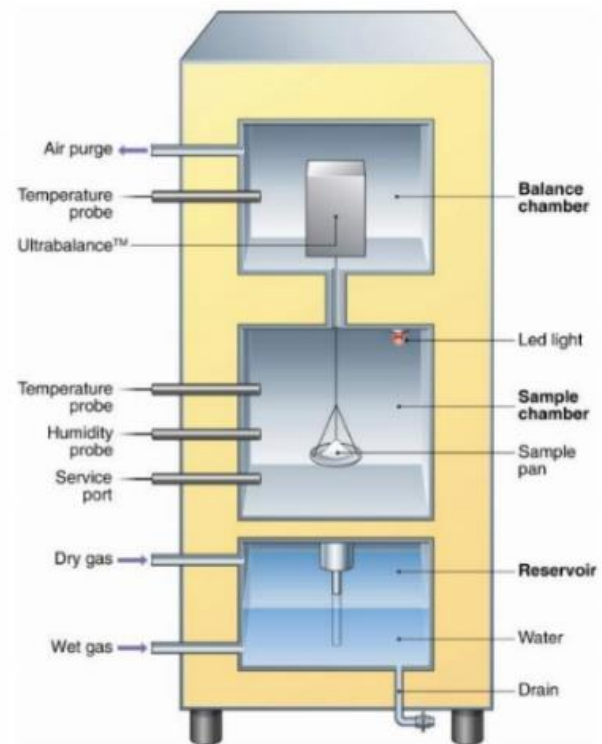


Figure 1 Schematic of the main components of the DVS Intrinsic (Surface Measurement Systems Company, 2023)

Table 1 DVS Intrinsic specifications (Surface Measurement Systems Company, 2023)

| Specifications | Values |
|---|------------------------|
| Temperature range (°C) | 20 - 40 |
| Temperature stability (°C) | +/-0.1 |
| Maximum mass (low/high mass instrument) (g) | 1 /4 |
| Mass change (low/high mass instrument) (g) | 0.150 - 1.0 |
| Stability (24 h at 25 °C and 0% RH) (low/high mass instrument) (µg) | < 5 - < 20 |
| Mass resolution (low/high mass instrument) (µg) | +/- 0.1 /1.0 |
| Humidity range | 0 - 98% |
| Relative humidity accuracy | +/-1% |
| Temperature stability (°C) | +/- 0.1 |
| Sample chamber (largeur × profondeur × hauteur) (mm) | 40 × 50 × 50 |
| Reservoir volume (mL) | 100 reservoir capacity |
| Mass (kg) | 22 |
| Size approximately (wide × deep × high) (cm) | 26 × 39 × 47 |
| Air supply (bar) | 3 to 4 |

2.3 Experimental procedure

The experiments are performed at 20 °C, 30 °C and 40 °C. In order for the software to automatically change the surrounding RH when moisture equilibrium for the sample is obtained, a dm/dt stability criterion must be met. The dm/dt stability criterion selected for the experiments is in the range

0.001%-0.002% /min and based on previous findings. For measuring the desorption isotherms with the DVS technique, samples of 2.5 mm thick are cut out from inside the blocks for each temperature. They are weighing from approx. 33.49 mg to approx. 36.23 mg, and subjected to desorption from water saturation. The desorption experiments are run starting at 90%

RH and ending at 0% RH in steps of 10% RH. The same procedure was followed by Engelund et al. (2010).

2.4 Modeling and statistical analysis of the water desorption curve of watermelon

Eleven theoretical models are tested in order to select the best model for describing the equation of the water desorption curve of watermelon. The experimental data are adjusted to the models and, to validate the goodness of the fit, six statistical criteria, namely correlation coefficient (r), coefficient of determination (R^2) to estimate regression reliability, standard error (SE), reduced chi-square (χ^2) to check model compatibility test, mean bias error (MBE) and root mean square error ($RMSE$) are calculated using Curve Expert Professional software (2.7.3) and MS Excel computer program. The relationship between the constants of the chosen model and the temperature is also determined and the effect of temperature on the constants of the equation is examined.

In other words, if we ignore the mathematical aspects of desorption curves, the study of the drying process can be significantly affected. Researchers in this context often repeat the use of mathematical models. However, models do not present the

diagnosis in the same way. Some of them exhibit better diagnostic accuracy than others. In addition, the use of many mathematical water desorption models is common, and comparing them allows to select the one that provides more insightful data. Choosing the most suitable model from a set of candidates can be guided by the model selection criteria, such as Reduced Chi-Squared, which measures the goodness of fit of a regression model, is used to measure the goodness of fit of the trained regression model on validation data sets. As the value of the calculated Reduced Chi-squared decreases, the observed data (experimental values) will be more similar to the expected data (predicted values by the model). The Experimental and predicted values are identical if the Reduced Chi-Square value is null. However, the experimental values differ from the predicted ones when the Reduced Chi-squared is higher. Consequently, the model with the smallest values of the Reduced Chi-Squared, is the most suitable.

Models used in this investigation are reported in Table 2. They express the equilibrium moisture content (X_{eq} , in kg H₂O/kg dry matter) of the fruit according to its water activity (a_w). X_{eq} represents the moisture level at which a dried fruit reaches a balance with its surrounding environment.

Table 2 Mathematical models applied to the water desorption isotherms

| Model | Equation | Reference | |
|---------------------|---|-------------------------------|------|
| Langmuir | $X_{eq} = A a_w / (1+B a_w)$ | (Langmuir, 1918) | (1) |
| BET | $X_{eq} = X_m \times C \times a_w / [(1-a_w)+(C-1)(1-a_w) \cdot a_w]$ | (Brunauer et al.,1938) | (2) |
| Oswin | $X_{eq} = A \times [a_w / (1-a_w)]^B$ | (Oswin, 1946) | (3) |
| Smith | $X_{eq} = A - B \ln(1-a_w)$ | (Smith, 1947) | (4) |
| Halsey | $X_{eq} = [-\exp(A)/\ln(a_w)]^{(1/B)}$ | (Halsey, 1948) | (5) |
| Henderson | $X_{eq} = [-\ln(1- a_w)/A]^{(1/B)}$ | (Henderson, 1952) | (6) |
| Kuhn | $X_{eq} = [C/\ln(a_w)]+k$ | (Kühn, 1964) | (7) |
| Chung-Pfost | $X_{eq} = 1/B \times [\ln(A) - \ln(-\ln(a_w))]$ | (Chung and Pfost, 1967) | (8) |
| Iglesias & Chirifie | $X_{eq} = A+B \times [a_w / (1- a_w)]$ | (Iglesias and Chirifie, 1978) | (9) |
| GAB | $X_{eq} = X_m \times C \times K \times a_w / [(1-k \times a_w) \times (1+(C-1) K a_w)]$ | (Van den Berg, 1984) | (10) |
| Lewicki | $X_{eq} = A/(1- a_w)^B - B/(1- a_w)^C$ | (Lewicki, 2000) | (11) |

The correlation coefficient (r) is calculated from Equation 12 (Amini et al., 2021):

$$r = \sqrt{1 - \frac{\sum_{i=1}^N [O_i - T_i]^2}{\sum_{i=1}^N [O_i - T_m]^2}} \tag{12}$$

The reduced chi-square (χ^2) is calculated with the degree of freedom which equals the number of observations N minus the number of fitted parameters

from Equation 13 (Sacilik and Elicin, 2006) :

$$\chi^2_{N-n} = \frac{\sum_{i=1}^N (O_i - T_i)^2}{N - n} \tag{13}$$

The mean bias error (MBE) is calculated from Equation 14 (Ukhurebor et al., 2020) :

$$MBE = \frac{1}{N} \sum_{i=1}^N (O_i - T_i) \tag{14}$$

The root mean square error ($RMSE$) is calculated

from Equation 15 (Sacilik and Elicin, 2006) :

$$RMSE = \left[\frac{1}{N} \sum_{i=1}^N (O_i - T_i)^2 \right]^{1/2} \quad (15)$$

Where: O_i is the i^{th} actual value (experimental), T_i is the i^{th} predicted value, N is the number of data, n is the number of constants and T_m is given by Equation 16 (Amini et al., 2021):

$$T_m = \sqrt{\frac{\sum_{i=1}^N O_i}{N}} \quad (16)$$

2.5 Determination of the desorption isosteric heat

In order to evaluate the water binding force to watermelon and in order to determine the required energy removing the water from the fruit during desorption, the calculation of the isosteric heat (Q_{st}) in kJ mol^{-1} , is essential (Koocheki et al., 2007). At each water content, Q_{st} can be calculated from Equation 17 (Chung and Pfof, 1967; Van den Berg, 1984).

$$Q_{st} = q_{st} + L_v \quad (17)$$

Where : q_{st} is the net isosteric heat of desorption in kJ mol^{-1} and L_v is the latent heat of vaporization of pure water in kJ mol^{-1} , calculated from Equation 18 (Iglesias and Chirife, 1978) :

$$L_v = R \times (6887 - 5.31T) \quad (18)$$

Where : R is the universal ideal gas constant = $8.315 \text{ J mol}^{-1} \text{ K}^{-1}$ and T is the average desorption temperature in K.

The net isosteric heats (q_{st}) with constant equilibrium water contents are calculated from the isosteric desorption curves. These curves are derived from the desorption isotherms previously found and illustrate the relationship between the water activity of the fruit and the constant water content temperature. To do this, the Clausius-Clapeyron equation applied to the desorption curves determined at three temperatures is used as follows (Basu et al., 2006; Chung and Pfof, 1967; Van den Berg, 1984) :

$$\frac{\delta \ln(a_w)}{\delta T} = \frac{q_{st}}{RT^2} \quad (19)$$

By integrating Equation 19, assuming that the water content is constant and the net desorption isosteric heat (q_{st}) is independent of temperature,

Equation 20 (Basu et al., 2006; Chung and Pfof, 1967) is obtained:

$$\ln(a_w) = -\frac{q_{st}}{R} \cdot \frac{1}{T} + k \quad (20)$$

Where: k is a constant and $(-q_{st}/R)$ is the slope of the curve $\ln(a_w) = f(1/T)$ with constant water content from which the net desorption isosteric heat can be calculated.

3 Results and discussion

3.1 DVS isotherm analysis

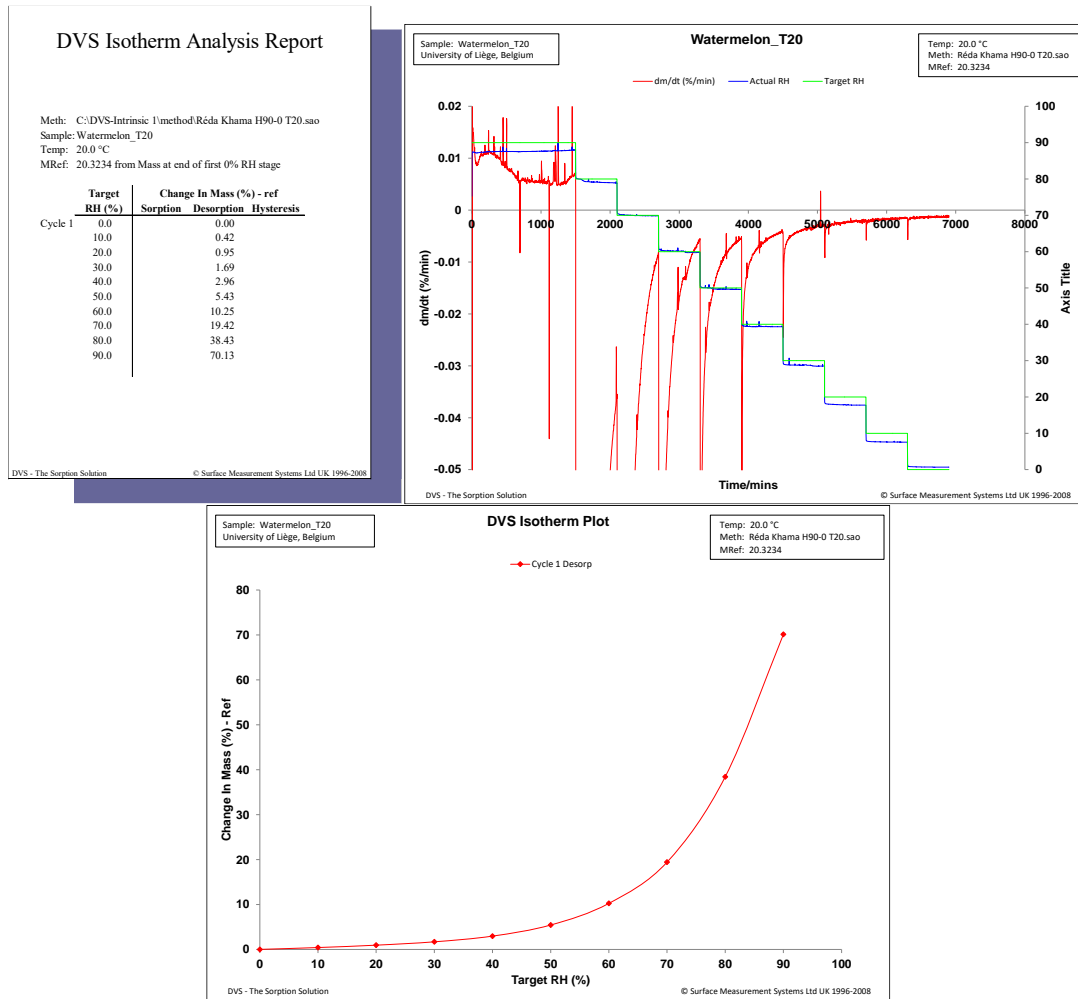
The schema of desorption measurement using the DVS is shown in Figure 2(a-c) and is prepared on the basis of the user's manual provided by the manufacturer. Then the basic results obtained from the desorption isotherm experiment are shown. The mass as function of time is illustrated along with the RH surrounding the fruit sample (Engelund et al., 2010). The graphs showing the courses of DVS, registered directly during the measurements, are presented. In Figure 2(a-c), it is shown how the courses of the researched desorption processes look like for the selected samples for 20 °C, 30 °C and 40 °C.

Due to the small sample amount used, i.e. only 35 mg dry mass, the entire experiment is completed within 2.5 days. The DVS isotherm analysis reports for three temperatures (20 °C, 30 °C and 40 °C) are shown in Figure 2(a), and the mass of watermelon sample and RH (dashed line) in the DVS equipment as function of time are shown in Figure 2(b). The change in mass over time can also be illustrated as the dm/dt over time in Figure 2(c) for three temperatures. As can be seen, the software automatically moves to the next RH step upon meeting the dm/dt stability criterion set by the operator. From Figure 2(b) and Figure 2(c) it is clear that the chosen criterion is satisfactory in securing a sample mass sufficiently close to the true equilibrium mass at the different RH levels. Thus, in the following the sample mass at the end of each RH step is referred to as the mass in equilibrium with the given climate conditions. This mass can be used for calculating the moisture content of the sample on the basis of the acquired dry mass of

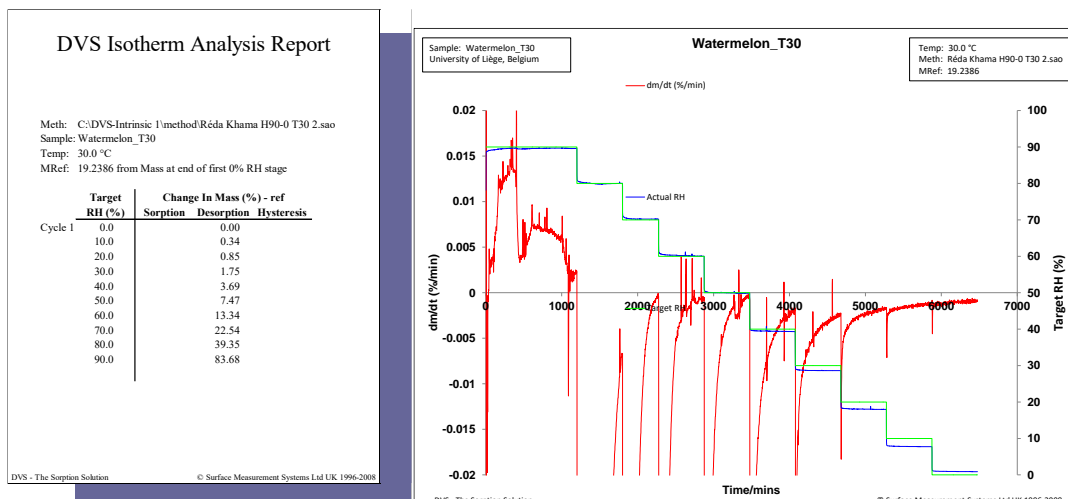
the sample. This is found after completing the first step of the test run at 0% RH (Figure 2(c)) (Engelund et al., 2010).

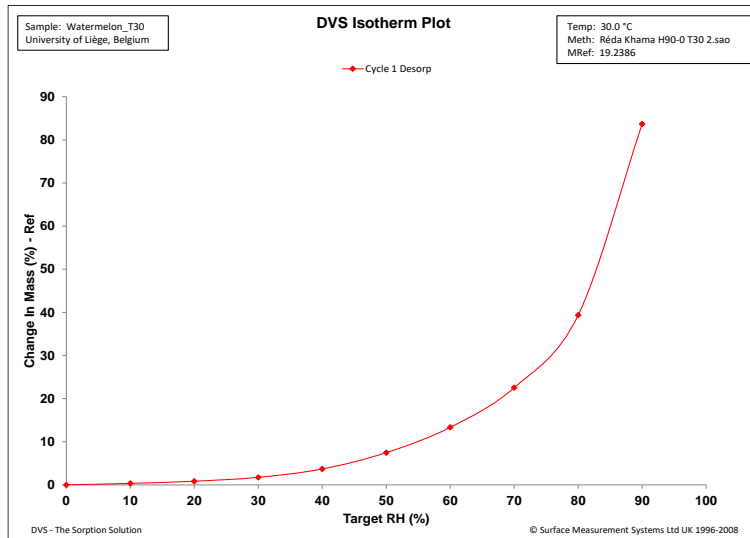
The water desorption curves of the watermelon at 20 °C, 30 °C and 40 °C, representing the equilibrium water content variation vs the water activity (RH of the air in equilibrium) are obtained via the DVS after an average of 4.5 days. According to the analysis, at

standard settings and automatic humidity changes at lower RH levels, mass equilibrium states have been obtained. However, for the highest humidities, it would be advisable to have typical DVS settings with a longer measurement time to ensure stabilization of the moisture equilibrium state in the fruit sample. The same findings were made by Garbalińska et al. (2017).

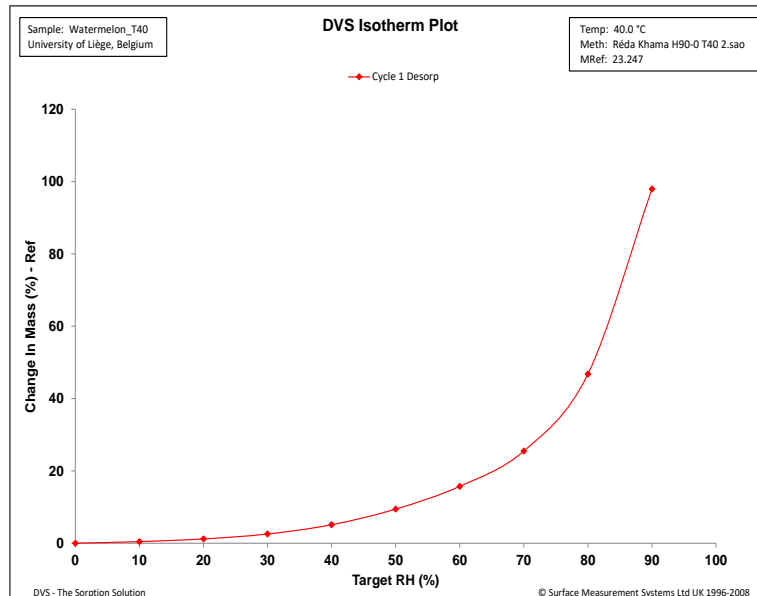
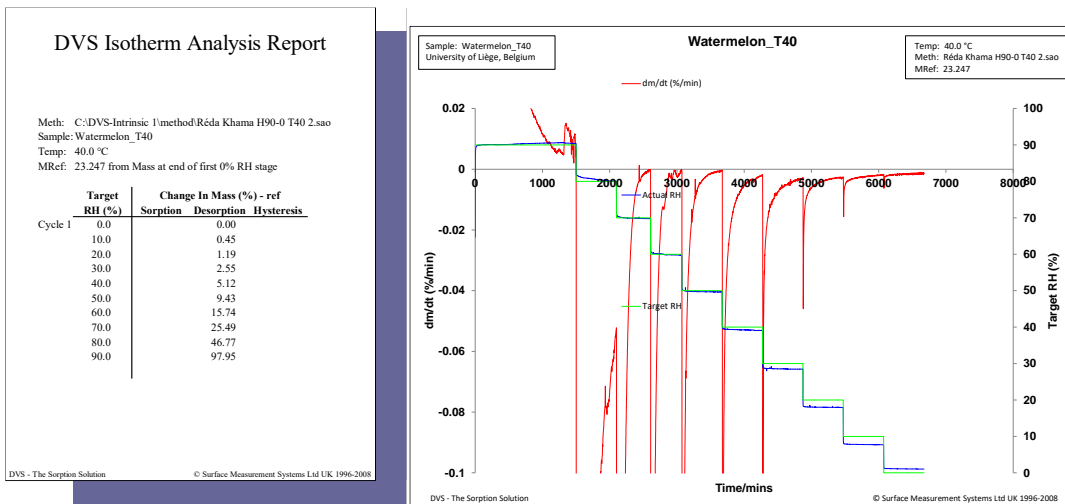


(a) DVS isotherm analysis report at 20°C





(b) Mass of watermelon sample and relative humidity (dashed line) in the DVS equipment as function of time



c) Mass change over time, dm/dt along with the relative humidity illustrated as function of time for the watermelon sample

Figure 2 Graphs showing the courses of DVS measurements for samples of watermelon at 20 °C, 30 °C and 40 °C

3.2 Influence of relative humidity and effect of temperature on the equilibrium water content of watermelon

Figure 3 shows the three desorption isotherms of watermelon at the temperature range of study. Since water and sugars are the main components of the

fruits (Basu et al., 2006), all the curves determined are of type III, according to the classification of Brunauer et al. Reported by (Basu et al., 2006; Lewicki, 2000). Contrary to popular belief, glucose and fructose are found in larger quantities in tomatoes, according to the USDA (USDA, 2015) nutrition laboratory. As for watermelon, the amount of sugars is even greater (USDA, 2015).

The equilibrium moisture content varies from 1.20×10^{-5} to 0.46, from 1.14×10^{-5} to 0.39 and from 1.67×10^{-5} to 0.35 $\text{kg water} \cdot \text{kg dry matter}^{-1}$ for the temperatures of 20 °C, 30 °C and 40 °C, respectively.

The effect of the temperature becomes perceptible from water activity values superior to 0.4.

In the range 0-0.4 of water activity, the equilibrium water content decreases at constant RH if temperature increases. This corresponds to the increase in the kinetic energy of the water molecules of the fruit, which leads to the reduction of attraction forces (Uribe et al., 2011). According to Deshmukh et al. (2017), this tendency can be explained by the consideration of the stirring states of the molecules. Similar results were obtained by Basu et al. (2006), and Uribe et al. (2011).

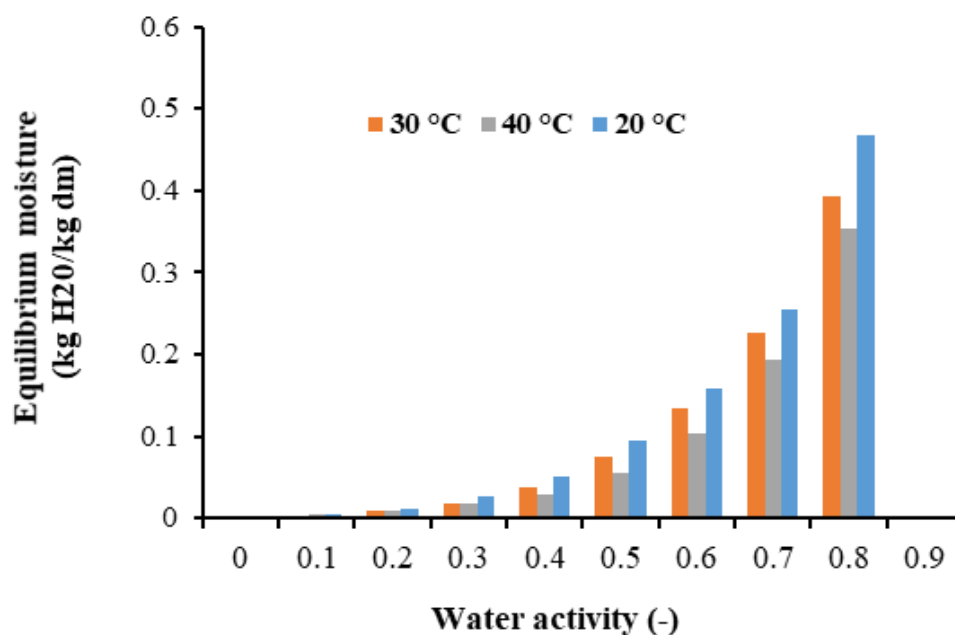


Figure 3 Isotherms desorption of watermelon at 20 °C, 30 °C and 40 °C, determined by using the DVS technique

3.3 Modeling results

The models statistical analyzes applied to the water desorption data, expressing changes in equilibrium water content as a function of water activity, are compared using the correlation coefficient, the coefficient of determination, the standard error, the reduced chi-squared, the mean bias error and the root mean square error; they are predicted by a non-linear regression analysis using the Curve Expert software and MS Excel computer program. They show that the Henderson model is the most appropriate model for the water desorption. The results are then summarized in Table 3. Halsey, Kuhn and Chung-Pfost models have failed catastrophically, and are not available. To take into account the

temperature effect on the two parameters (A and B) of the selected Henderson model, the values are examined for all the tests carried out. It appears that the variations of A and B are negligible in the interval 20 °C-40 °C and therefore each parameter is taken as a constant. Indeed, the proposed values for A and B are 2.52 and 0.49, respectively (Table 4).

The validation of the Henderson model is performed by comparing the calculated water contents (predicted values) with experimentally determined values. This comparison is illustrated in Figure 4. The model predictions and the desorption data around a line show the relevance of the selected model in the description of the water desorption behavior of the fruit.

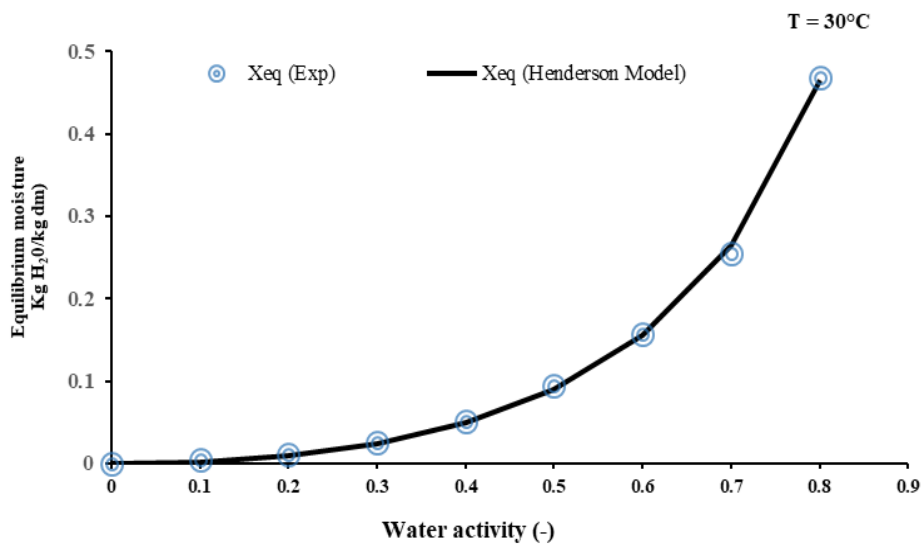
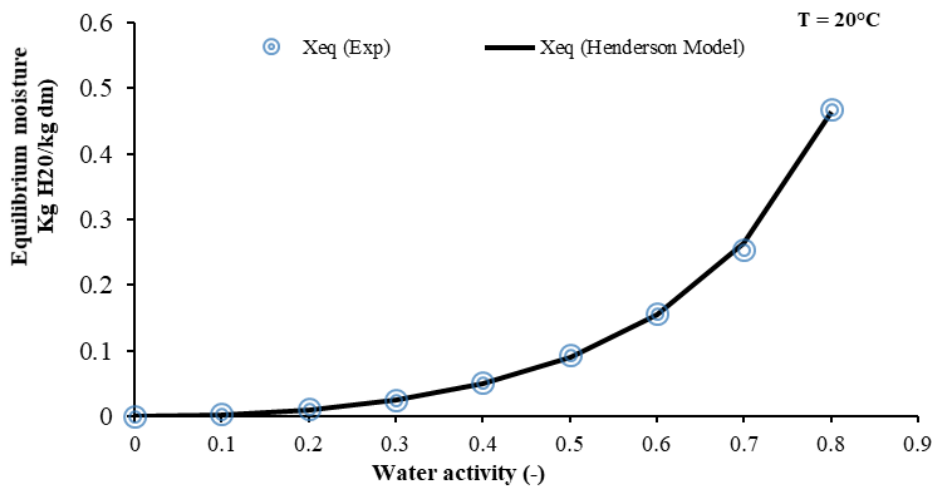
Table 3 Statistics of mathematical models applied to the water desorption isotherms of watermelon

| Models | T (°C) | R ² | SE | χ ² | MBE | RMSE |
|-----------------------|-----------|----------------|---------------|----------------|----------------|---------------|
| Langmuir | 20 | 0.9964 | 0.0099 | 0.00009 | -0.0037 | 0.0087 |
| | 30 | 0.9919 | 0.0127 | 0.00016 | -0.0045 | 0.0112 |
| | 40 | 0.9923 | 0.0110 | 0.00012 | -0.0033 | 0.0097 |
| BET | 20 | 0.9985 | 0.0062 | 0.00004 | -0.0019 | 0.0055 |
| | 30 | 0.9958 | 0.0091 | 0.00008 | -0.0026 | 0.0081 |
| | 40 | 0.9971 | 0.0067 | 0.00004 | -0.0015 | 0.0060 |
| Oswin | 20 | 0.9986 | 0.0061 | 0.00004 | 0.0017 | 0.0054 |
| | 30 | 0.9957 | 0.0092 | 0.00009 | 0.0023 | 0.0082 |
| | 40 | 0.9971 | 0.0067 | 0.00005 | 0.0011 | 0.0060 |
| Smith | 20 | 0.9199 | 0.0471 | 0.00222 | 0.0336 | 0.0416 |
| | 30 | 0.9194 | 0.0404 | 0.00163 | 0.0142 | 0.0357 |
| | 40 | 0.8924 | 0.0416 | 0.00173 | 0.0040 | 0.0367 |
| Anderson | 20 | 0.9993 | 0.0043 | 0.00001 | 0.0008 | 0.0038 |
| | 30 | 0.9997 | 0.0026 | 0.00001 | -0.0003 | 0.0023 |
| | 40 | 0.9993 | 0.0034 | 0.00001 | 0.0008 | 0.0030 |
| Iglesias and Chirifie | 20 | 0.9961 | 0.0102 | 0.00011 | -0.00004 | 0.0091 |
| | 30 | 0.9944 | 0.0106 | 0.00011 | 0.00005 | 0.0094 |
| | 40 | 0.9881 | 0.0138 | 0.00020 | -0.00001 | 0.0122 |
| GAB | 20 | 0.9991 | 0.0057 | 0.00002 | -0.0014 | 0.0043 |
| | 30 | 0.9973 | 0.0085 | 0.00005 | -0.0025 | 0.0064 |
| | 40 | 0.9979 | 0.0067 | 0.00003 | -0.0013 | 0.0050 |
| Lewicki | 20 | 0.9989 | 0.0057 | 0.00003 | -0.0002 | 0.0047 |
| | 30 | 0.9968 | 0.0086 | 0.00006 | -0.0003 | 0.0070 |
| | 40 | 0.9971 | 0.0073 | 0.00005 | -0.0001 | 0.0060 |

Table 4 Mathematical models parameters

| Models | T (°C) | Parameters | SE | Range (95% confidence) |
|-----------------------|--------|-------------------------|--------|------------------------|
| Langmuir | 20 | A = 0.0920 | 0.0050 | 0.0801 to 0.1038 |
| | | B = -1.0543 | 0.0122 | -1.0834 to -1.0253 |
| | 30 | A = 0.0784 | 0.0064 | 0.0630 to 0.0937 |
| | | B = -1.0528 | 0.0188 | -1.0973 to -1.0084 |
| | 40 | A = 0.0613 | 0.0050 | 0.0493 to 0.0734 |
| | | B = -1.0785 | 0.0161 | -1.1167 to -1.0402 |
| BET | 20 | X _m = 0.1428 | 0.0064 | 0.1275 to 0.1582 |
| | | C = 0.4814 | 0.0530 | 0.3559 to 0.6069 |
| | 30 | X _m = 0.1227 | 0.0098 | 0.0993 to 0.1460 |
| | | C = 0.4655 | 0.0893 | 0.2543 to 0.6768 |
| | 40 | X _m = 0.1290 | 0.0115 | 0.1018 to 0.1563 |
| | | C = 0.3121 | 0.0553 | 0.1812 to 0.4429 |
| Oswin | 20 | A = 0.0932 | 0.0029 | 0.0863 to 0.1001 |
| | | B = 1.1681 | 0.0256 | 1.1074 to 1.2289 |
| | 30 | A = 0.0781 | 0.0043 | 0.0677 to 0.0885 |
| | | B = 1.1776 | 0.0459 | 1.0689 to 1.2863 |
| | 40 | A = 0.0614 | 0.0031 | 0.0539 to 0.0689 |
| | | B = 1.2731 | 0.0414 | 1.1751 to 1.3711 |
| Smith | 20 | A = -0.0553 | 0.0249 | -0.1144 to 0.0036 |
| | | B = 0.2786 | 0.0310 | 0.2051 to 0.3521 |
| | 30 | A = -0.0495 | 0.0214 | -0.1001 to 0.0011 |
| | | B = 0.2383 | 0.0266 | 0.1752 to 0.3013 |
| | 40 | A = -0.0455 | 0.0220 | -0.0977 to 0.0065 |
| | | B = 0.2092 | 0.0274 | 0.1443 to 0.2741 |
| Anderson | 20 | A = 2.3862 | 0.0227 | 2.3325 to 2.4399 |
| | | B = 0.5135 | 0.0083 | 0.4937 to 0.5333 |
| | 30 | A = 2.5825 | 0.0197 | 2.5359 to 2.629129 |
| | | B = 0.5089 | 0.0059 | 0.4948 to 0.522985 |
| | 40 | A = 2.6004 | 0.0284 | 2.5331 to 2.6676 |
| | | B = 0.4636 | 0.0079 | 0.4447 to 0.4825 |
| Iglesias and Chirifie | 20 | A = -0.0176 | 0.0046 | -0.0286 to -0.0065 |
| | | B = 0.1191 | 0.0027 | 0.1125 to 0.1257 |

| | | | | |
|----------------|------------|----------------|-----------------------------|-----------------------------|
| GAB | 30 | A = -0.0171 | 0.0048 | -0.0286 to -0.0056 |
| | | B = 0.1018 | 0.0028 | 0.0949 to 0.1086 |
| | 40 | A = -0.0183 | 0.0062 | -0.0332 to -0.0034 |
| | | B = 0.0904 | 0.0037 | 0.0815 to 0.0993 |
| | 20 | $X_m = 0.2352$ | 314096.8928 | -807411.5325 to 807412.0030 |
| | | C = 0.2341 | 239873.0900 | -616613.1742 to 616613.6425 |
| | | K = 1.1056 | 343464.1160 | -882901.5126 to 882903.7237 |
| | | k = 0.8467 | 10118.0574 | -26008.4478 to 26010.1413 |
| | | $X_m = 0.1893$ | 455410.8049 | -1170670,554 to 1170670,932 |
| | | C = 0.2435 | 441459.0074 | -1134806,262 to 1134806,749 |
| | 30 | K = 1.1193 | 663470.6788 | -1705504.556 to 1705506.795 |
| | | k = 0.8467 | 8921.3035 | -22932,0942 to 22933,7876 |
| $X_m = 1.0166$ | | 2772066.2358 | -7125822.099 to 7125824.132 | |
| C = 0.0404 | | 105744.5598 | -271825.004 to 271825.085 | |
| 40 | | K = 0.9229 | 102901.5448 | -264515.919 to 264517.765 |
| | | k = 0.8855 | 2097.21930 | -5390.188 to 5391.959 |
| 20 | A = 0.8044 | 0.0433 | 0.6983 to 0.9106 | |
| | B = 0.8120 | 0.0408 | 0.7122 to 0.9118 | |
| | C = 0.6995 | 0.0563 | 0.5615 to 0.8374 | |
| | 30 | A = 0.7697 | 0.0731 | 0.5907 to 0.9486 |
| | | B = 0.7794 | 0.0692 | 0.6099 to 0.9488 |
| | | C = 0.6726 | 0.0942 | 0.4420 to 0.9031 |
| 40 | A = 0.9216 | 0.0857 | 0.7117 to 1.1315 | |
| | B = 0.9272 | 0.0824 | 0.7253 to 1.1290 | |
| | C = 0.8667 | 0.0979 | 0.6270 to 1.1064 | |



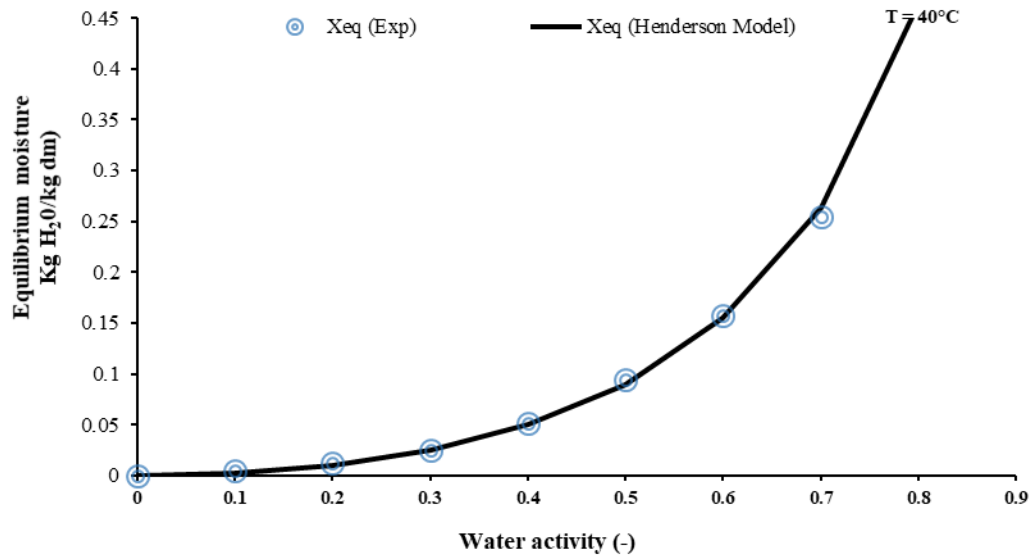


Figure 4 Experimental and predicted (Henderson model) desorption isotherms of watermelon

3.4 Determination of the desorption isosteric heat of watermelon

By plotting the curves $\ln(a_w) = f(1/T)$, the affine lines obtained in Figure 5 are the desorption isosteres of watermelon. This figure already shows that the isosteres slopes become weaker as the equilibrium water contents decrease. In other words, the net isosteric heats of desorption are inversely proportional to the equilibrium water contents

because the lines slopes are always negative (Equation 20). Similar results have been reported by other authors (Basu et al., 2006; Koocheki et al., 2007; Nur Farah Hani et al., 2014; Kiranoudis et al., 1993).

The isosteric equations obtained and used for the determination of the net isosteric heats (q_{st}) are summarized in Table 5. The determination coefficients of all elaborated regressions are close to 1, thus showing an excellent correlation.

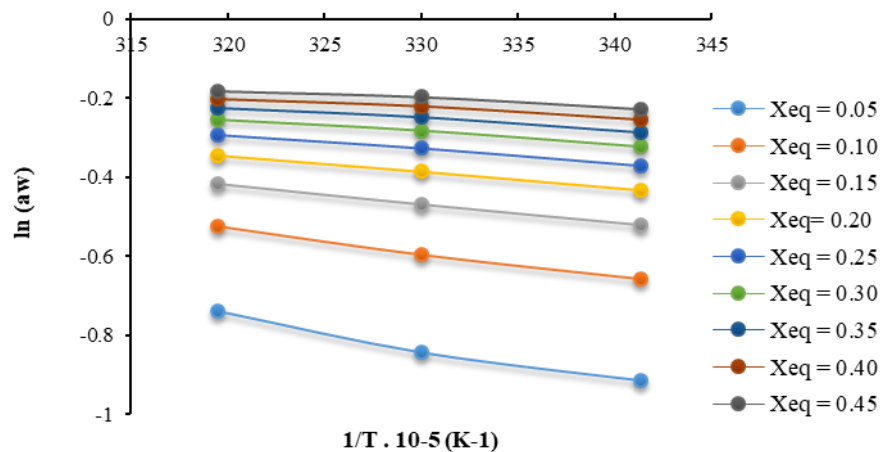


Figure 5 Desorption isosteres of watermelon

Table 5 Isosteric equations of watermelon

| $X_{eq}, \text{kg H}_2\text{O} / \text{kg dry matter}$ | Equation | k | R^2 |
|--|-------------------------|--------|--------|
| 0.45 | $y = -0.0022x + 0.5297$ | 0.5297 | 0.9686 |
| 0.40 | $y = -0.0025x + 0.5874$ | 0.5874 | 0.9777 |
| 0.35 | $y = -0.0028x + 0.6556$ | 0.6556 | 0.9855 |
| 0.30 | $y = -0.0031x + 0.7374$ | 0.7374 | 0.9920 |
| 0.25 | $y = -0.0035x + 0.8379$ | 0.8379 | 0.9968 |
| 0.20 | $y = -0.0041x + 0.9653$ | 0.9653 | 0.9996 |
| 0.15 | $y = -0.0049x + 1.1346$ | 1.1346 | 0.9996 |
| 0.10 | $y = -0.0060x + 1.3784$ | 1.3784 | 0.9954 |
| 0.05 | $y = -0.0080x + 1.7940$ | 1.7940 | 0.9831 |

The isosteric heats (Q_{st}) of the watermelon are calculated using Equation 18 and plotted as a function of the equilibrium water content in Figure 6. In addition to the variation of (Q_{st}) as a function of (X_{eq}), this figure also shows the variation of (q_{st}) as a function of the same explanatory variable and gives the possibility of comparing the two variables explained with the latent heat of vaporization of the pure water (L_v). Figure 6 shows that the isosteric heat is more important for low moistures and, for high humidities, it becomes negligible in front of latent heat of evaporation. Going from 0.05 to 0.45 kg water.kg dry matter⁻¹ of equilibrium moisture content, the values of isosteric heat vary from 65.02 to 113.25 kJ mol⁻¹.

The difference between the isosteric (Q_{st}) and the net isosteric (q_{st}) heats of desorption remains constant whatever the value of the water content, the difference is the latent heat of vaporization. The difference between the isosteric heat (Q_{st}) and the latent heat of vaporization (L_v) decreases as the moisture content increases to zero at high water content values. Therefore, the value of the isosteric heat tends towards the latent heat value. This is due to the decrease in the net desorption isosteric heat which tends to zero at the high water content values. In order to express the isosteric heat (Q_{st}) as a function of the equilibrium water content, the following equation is proposed:

$$Q_{st} = 110 \exp(-1.29 X_{eq}) \quad (21)$$

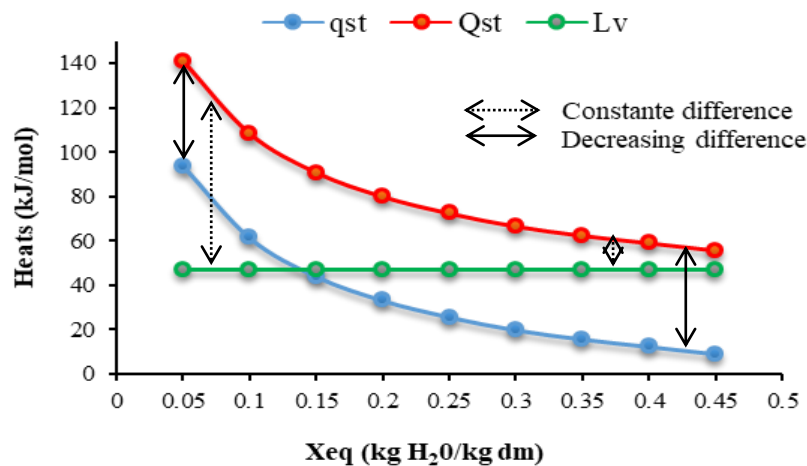


Figure 6 Temperature effect on the isosteric heat of watermelon

4 Conclusion

The study of the water desorption of watermelon by a gravimetric method using DVS has shown the success of such a method for the experimental determination of the equilibrium water contents of fruits. Contrary to the long durations taken for the determination of the water desorption isotherms of fruits by the static method, four and a half days are largely sufficient to reach equilibrium via DVS. The main results can be summarized as follows:

The results show that the Henderson model is the most appropriate model to represent the water desorption of watermelon fruit and the obtained curves are of the type III.

In the range 0-0.8 of the water activity, the

equilibrium moisture content average of watermelon varies from 1.20×10^{-5} to 0.46, from 1.14×10^{-5} to 0.39 and from 1.67×10^{-5} to 0.35 kg water.kg dry matter⁻¹ at the temperatures of 20 °C, 30 °C and 40 °C, respectively.

At constant temperature, the equilibrium moisture content increases with water activity and there is no influence of the temperature on desorption in the interval 0-0.4 of water activity.

At constant RH, the equilibrium moisture content is inversely proportional to the temperature in the interval 0-0.4 of water activity.

The net isosteric heat of desorption is inversely proportional to the equilibrium moisture content and becomes negligible in front of the evaporation latent heat for the high humidities. In the interval 0.05 - 0.45 kg water.kg dry matter⁻¹ of equilibrium moisture, the

isosteric heat values vary from 65.02 to 113.25 kJ mol⁻¹.

References

- Amini, G., F. Salehi, and M. Rasouli. 2021. Drying kinetics of basil seed mucilage in an infrared dryer: Application of GA-ANN and ANFIS for the prediction of drying time and moisture ratio. *Journal of Food Processing and Preservation*, 45(3): e15258.
- Anderberg, A., and L. Wadsö. 2008. Method for simultaneous determination of sorption isotherms and diffusivity of cement-based materials. *Cement and Concrete Research*, 38(1): 89-94.
- Argyropoulos, D., R. Alex, and J. Müller. 2011. Equilibrium moisture contents of a medicinal herb (*Melissa officinalis*) and a medicinal mushroom (*Lentinula edodes*) determined by dynamic vapour sorption. *Procedia Food Science*, 1: 165-172.
- Arlabosse, P., E. Rodier, J. H. Ferrasse, S. Chavez, and D. Lecomte. 2003. Comparison between static and dynamic methods for sorption isotherm measurements. *Drying Technology*, 21(3): 479-497.
- Basu, S., U. S. Shivhare, and A. S. Mujumdar. 2006. Models for sorption isotherms for foods: A review. *Drying Technology*, 24(8): 917-930.
- Bingol, G., B. Prakash, and Z. Pan. 2012. Dynamic vapor sorption isotherms of medium grain rice varieties. *LWT - Food Science and Technology*, 48(2): 156-163.
- Brunauer, S., P. H. Emmett, and E. Teller. 1938. Adsorption of gases in multi molecular layers. *Journal of the American Chemical Society*, 60(2): 309-319.
- Caballero-Cerón, C., J. A. Guerrero-Beltrán, H. Mújica-Paz, J. A. Torres, and J. Welti-Chanes. 2015. Moisture Sorption Isotherms of Foods: Experimental Methodology, Mathematical Analysis, and Practical Applications. In *Water Stress in Biological, Chemical, Pharmaceutical and Food Systems*, eds. Gutiérrez-López, G., L. Alamilla-Beltrán, M. del Pilar Buera, J. Welti-Chanes, E. Parada-Arias, and G. Barbosa-Cánovas, ch. 15, 187-214. New York, NY, USA: Springer.
- Chung, D. S., and H. B. Pfost. 1967. Adsorption and desorption of water vapour by cereal grains and their products. Part I. Heat and free energy changes of adsorption and desorption. *Transactions of the ASAE*, 10(4): 549-551.
- Deshmukh, G., P. Birwal, S. Patel, R. Datir, and A. Surywanshi. 2017. Sorption isotherms of traditional Indian dairy products: A review. *Journal of Food, Nutrition and Population Health*, 1(3): 25.
- Djendoubi Mrad, N., C. Bonazzi, N. Boudhrioua, N. Kechaou, and F. Courtois. 2012. Influence of sugar composition on water sorption isotherms and on glass transition in apricots. *Journal of Food Engineering*, 111(2): 403-411.
- Djendoubi Mrad, N., C. Bonazzi, F. Courtois, N. Kechaou, and N. Boudhrioua Mihoubi. 2013. Moisture desorption isotherms and glass transition temperatures of osmo-dehydrated apple and pear. *Food and Bioprocess Technology*, 91(2): 121-128.
- Engelund, E. T., M. Klamer, and T. M. Venås. 2010. Acquisition of sorption isotherms for modified woods by the use of dynamic vapour sorption instrumentation. Principles and Practice. In *the International Research Group on Wood Protection, 41st Annual Meeting, IRG/WP 10-40518*. Biarritz, France, 9-13 May.
- Garbalińska, H., M. Bochenek, W. Malorny, and J. van Werder. 2017. Comparative analysis of the dynamic vapor sorption (DVS) technique and the traditional method for sorption isotherms determination - Exemplified at autoclaved aerated concrete samples of four density classes. *Cement and Concrete Research*, 91: 97-105.
- Goula, A. M., T. D. Karapantsios, D. S. Achilias, and K. G. Adamopoulos. 2008. Water sorption isotherms and glass transition temperature of spray dried tomato pulp. *Journal of Food Engineering*, 85(1): 73-83.
- Halsey, G. 1948. Physical adsorption on non-uniform surfaces. *The Journal of Chemical Physics*, 16(10): 931-937.
- Haoua, A., A. Leonard, and B. Bouchekima. 2015. Determination of desorption isotherms using the DVS apparatus (dynamic vapor sorption system) at different temperatures on unblanched and blanched samples of potato. *Journal of Agroalimentary Processes and Technologies*, 21(2): 142-147.
- Henderson, S. M. 1952. A basic concept of equilibrium moisture. *Agricultural Engineering*, 33: 29-32.
- Iglesias, H. A., and J. Chirife. 1978. An empirical equation for fitting water sorption isotherms of fruits and related products. *Canadian Institute of Food Science and Technology Journal*, 11(1): 12-15.
- Kerje, T., and M. Grum. 2000. The origin of melon, *Cucumis melo*: A review of the literature. *Acta Horticulturae*, 510: 37-44.
- Khama, R. 2016. Conception, réalisation et simulation d'un séchoir solaire opérant en mode convectif utilisé pour le séchage de produits agroalimentaires. Ph.D. diss., Département de Génie des procédés. Université Abderrahmane Mira Bêjaia (UAMB), Algérie.
- Kiranoudis, C. T., Z. B. Maroulis, E. Tsami, and D. Marinou-Kouris. 1993. Equilibrium moisture content and heat of desorption of some vegetables. *Journal of Food*

- Engineering*, 20(1): 55-74.
- Koocheki, A., S. M. A. Razavi, E. Milani, T. M. Moghadam, M. Abedini, S. Alamatyan, and S. Izadkhah. 2007. Physical properties of watermelon seed as a function of moisture content and variety. *International Agrophysics*, 21(4): 349-359.
- Kühn, I. 1964. A new theoretical analysis of adsorption phenomena: Introductory part: The characteristic expression of the main regular types of adsorption isotherms by a simple equation. *Journal of Colloid Science*, 19(8): 685-698.
- Langmuir, I. 1918. The adsorption of gases on plane surfaces of glass, mica and platinum. *Journal of the American Chemical Society*, 40(9): 1361-1403.
- Lewicki, P. P. 2000. Raoult's law-based food water sorption isotherm. *Journal of Food Engineering*, 43(1): 31-40.
- Maoto, M. M., D. Beswa, and A. I. O. Jideani. 2019. Watermelon as a potential fruit snack. *International Journal of Food Properties*, 22(1): 355-370.
- Nur Farah Hani, M., W. Z. Wan Nur Zahidah, K. Saniah, and H. S. M. Irwani. 2014. Effects of drying on the physical characteristics of dehydrated watermelon rind candies. *Journal of Tropical Agriculture and Food Science*, 42(2): 115-123.
- Oswin, C. R. 1946. The kinetics of package life. III. Isotherm. *Journal of the Society of Chemical Industry*, 65(12): 419-421.
- Sacilik, K., and A. K. Elicin. 2006. The thin layer drying characteristics of organic apple slices. *Journal of Food Engineering*, 73(3): 281-289.
- Smith, S. E. 1947. The sorption of water vapour by high polymers. *Journal of the American Chemical Society*, 69(3): 646-651.
- Surface Measurement Systems Company. 2023. Advanced Sorption Analyzers: DVS Intrinsic PLUS Compact DVS instrument for complex water sorption challenges. Available at: <https://surfacemeasurementsystems.com/product/dvs-intrinsic-plus/>. Accessed on 19-06-2023 and 19-11-2023.
- Ukhurebor, K. E., S. O. Azi, U. O. Aigbe, R. B. Onyancha, and J. O. Emegha. 2020. Analyzing the uncertainties between reanalysis meteorological data and ground measured meteorological data. *Measurement*, 165: 108110.
- United State Department of Agriculture (USDA). 2015. Food and Nutrition. Available at: <https://www.usda.gov>. Accessed on 19-09-2015 and 05-03-2021.
- Uribe, E., A. Vega-Gálvez, K. Di Scala, R. Oyanadel, J. S. Torrico, and M. Miranda. 2011. Characteristics of Convective Drying of Pepino Fruit (*Solanum muricatum* Ait.): Application of Weibull Distribution. *Food and Bioprocess Technology*, 4: 1349-1356.
- Van den Berg, C. 1984. Desorption of water activity of foods for engineering purposes by means of the GAB model of sorption. In *Engineering and Foods (Vol. 1)*, ed. B. M. McKenna, 311-321. London, U.K.: Elsevier.
- Yang, R., J. Guan, S. Sun, S. S. Sablani, and J. Tang. 2020. Understanding water activity change in oil with temperature. *Current Research in Food Science*, 3: 158-165.